

# Waved Glass

## towards optimal light distribution on solar cell surfaces

### for high efficient modules

Luzi Bergamin and Tallha Sammarae  
*email: Luzi.Bergamin@esa.int*

**Abstract**—A method to improve the module efficiency of solar cells by modifying the surface of the glass cover of the solar cells module is presented. It is shown that a better efficiency can be achieved by a better distribution of incident light and secondarily by decreasing the (resistive) ohmic losses. This method is illustrated by taking industrial crystalline Silicon solar cells as an example. However, the method applies to all solar cells that are characterised by having a metallisation pattern at the surface of the solar cell. It is estimated that this method can improve the relative module efficiency by about 5%.

#### I. BACKGROUND

Crystalline Silicon solar cells are made of wafers with typical thickness between 100 and 200  $\mu\text{m}$  and square length from  $100 \times 100\text{mm}^2$  to  $300 \times 300\text{mm}^2$ . The wafers consist of two different doped layers; one is doped with Boron (p-Si) and represents the bulk of the solar cell, the other one, which is the sun facing side, is a Phosphorus doped (n-Si) layer as thin as 0.5  $\mu\text{m}$ . On top of this layer a silver front contact grid (metallisation pattern) is placed to collect the generated current when the solar cell is illuminated. The design of this contact grid has a certain pattern which should allow a maximum illumination, i.e. to cover as little area as possible by making the lines of the pattern as thin as possible. However, the front contact grid has a considerable ohmic resistance that contributes to power losses. Figure 1 below illustrates the schematic structure of the solar cell.

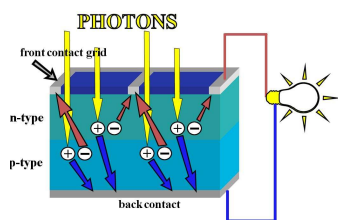


Fig. 1. A schematic view of typical crystalline solar cell[1]. The front contact grid consists of fingers that collect the current from the surface of the cell (this is indicated by the red arrows) and the bus bar which collect the current from the fingers.

In a conventional solar cells module, the solar cells are interconnected and covered with a protective flat glass as indicated in figure 2 (left hand side). Obviously the area under the front contact grid is not illuminated and does not contribute to power generation and thereby it contributes to loss in efficiency, so called shadow losses. The relative loss of efficiency due to

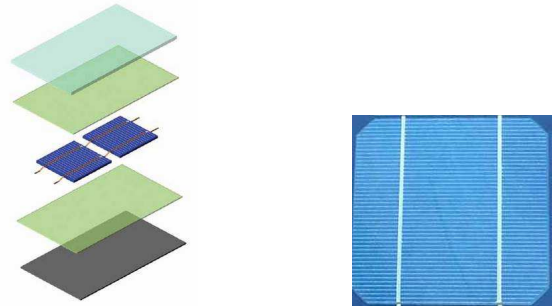


Fig. 2. Left: structural layers of a solar cells module with two sealing layers above and under the cells and a protective glass cover at the top [2]. Right: H-shape of front contact grid. The horizontal lines are the fingers and the two vertical lines are the bus bars.

this shadow is equal to the ratio of the total front contact grid area to the cell area. The typical front contact grid is an H-shape pattern as shown in figure 2 (right hand side). The contact fingers (horizontal lines) are typically 100  $\mu\text{m}$  wide and 15  $\mu\text{m}$  high. The bus-bars (vertical lines) are about 3 mm wide and 200  $\mu\text{m}$  high. The distance between the contact fingers is a key design parameter and is typically 2.2 mm for a  $156 \times 156$  mm square solar cell. The ohmic losses accrue due to current flowing through the emitter sheet (sheet resistance), the metal—semiconductor junction (contact resistance) and finally through the front contact grid (line resistance). If, for instant, the distance between the fingers is decreased, then the sheet resistance would be decreased because the current would have a shorter path through the emitter sheet. At the same time the line (finger) resistance would be decreased as there would be more lines available on the cell to transport the generated current. Similarly, if the number of fingers is increased, the contact area of metal—semiconductor junction is increased proportionally. Again this will reduce power losses due to contact resistance. Unfortunately, these advantages would be compensated by the shadow losses because of the increased number of fingers. It can be concluded that the optimal design of the cell is a result of a trade-off between shadow losses and ohmic losses. A novel method is presented here to reduce the shadow losses and simultaneously decrease the above mentioned ohmic losses.

## II. DESCRIPTION OF THE METHOD

Our approach is to modify the surface of the top glass layer (cf. figure 2). The modified surface works similar to a lens refracting the light over the front contact grid of the solar cell. The surface of the glass should take a certain shape such that the incident light over the fingers and bus-bars is refracted aside of the contact grid. In the optimal case no light would fall on the front contact grid and all the light would strike over the active area of the cell. In this optimal case the shadow loss would be eliminated altogether. However, the optimal case is difficult to achieve because it requires discontinuities in the slope of the top glass which might weaken the stiffness of the structure (cf. figure 3, top). Therefore a more practical approach will try to decrease the shadow losses without such discontinuities. Possible designs for both alternatives are depicted in figure 3, technical details on the design strategies are explained in appendix I.

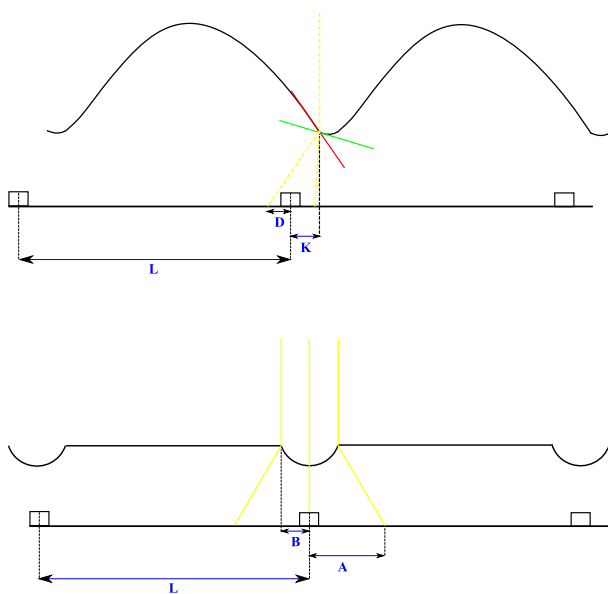


Fig. 3. Top: A possible design avoiding shadow losses completely. Notice the necessary discontinuity at a distance  $K$  from the fingers. Bottom: This design can avoid discontinuities, the apparent edges are not important and may be smoothed appropriately. For the sake of clarity the profile in both figures is distended.

The main potential of the method derives from the fact that the distance between the fingers can be decreased while keeping the shadow losses low. This means that there would be more fingers available on the cell to transport the generated current and this can decrease the ohmic losses caused by line, sheet and contact resistances.

### A. Potential of the method

In the following an estimate of the gain due to a waved glass is made, whereby the simpler design with a partial suppression of the shadow losses (cf. the design at the bottom of figure 3) is assumed. For any technical details appendix II should be consulted. The estimated relative efficiency losses for a standard flat glass are about 4% due to shadow of the fingers and about the same due to the bus-bar. The improvement due to

the reduction of the distance between the fingers is about 3% relative. The improvement in relative efficiency is estimated here by assuming that there is a concave shape (maximum width 0.5 mm) on the waved glass cover over the front contact grid area that diffracts the light by 10 Degrees away from the metallisation area. According to this assumption light intensity over the fingers is reduced to the factor of 0.33. This allows to reduce the distance between the fingers from 2.2 mm down to 1.4 mm. In table I a comparison of the different losses for a waved glass and a flat glass is made.

	Waved glass %	Flat Glass %	Gain %
Emitter losses	0.490	1.210	0.720
Line resistance losses	0.809	1.271	0.462
Contact losses	0.594	0.933	0.339
Total resistive losses	1.893	3.414	1.521
Shadow losses	2.357	4.545	2.188
Total losses	4.250	7.960	3.710
Gain from bus bar	1.320	-	1.320
Total improvement			5.030

TABLE I  
RESISTIVE AND SHADOW LOSSES OF A SOLAR CELL WITH A FLAT AND  
WAVED GLASS, RESP.

These calculations are based on a typical crystalline  $156 \times 156 \text{ mm}^2$  solar cell and a solar cells module incorporating a cover glass with a thickness of 3mm. The solar cell is assumed to have 15% efficiency under standard conditions, i.e.  $1000 \text{ W/m}^2$  and at  $25^\circ \text{C}$ . The typical values involved in the calculations are presented in table II.

Emitter sheet resistance	50	Ohm
Specific contact resistance	0.01	Ohm $\times \text{cm}^2$ $\leftrightarrow$ 50 Ohm sheet resistance
Specific line resistance	0.2	Ohm/cm $\leftrightarrow$ $100 \times 10 \mu\text{m}$ finger cross section
Length of unit cell	3.8	cm
Finger width	0.01	cm
Voltage at max. power point	0.55	V
Current generation	0.033	A/cm $^2$

TABLE II  
TYPICAL VALUES OF A CRYSTALLINE SOLAR CELLS UNDER STANDARD  
TEST CONDITIONS.

The estimated values in table I are only valid if the illumination source (sun) is perpendicular to the surface of the cell. If this is not the case, then the regions of low and high intensity shown in figure 3 will be displaced which will reduce the efficiency. However, it is possible to put the solar cells in a certain orientation to reduce efficiency losses when the sun is not perpendicular to the cells. Let us consider the front grid contact again; it consist for bus bars that vertical to the fingers. According to table I, the gain in efficiency is mainly due to the waved glass structure along the fingers. It is possible to orient the cell such that the sun is nearly always perpendicular to the bus bar. In this configuration when the sun moves from east to west the displacement of the mentioned high and low illumination is minimised, but there will be no gain from the waved structure over the bus bar. In this case, the minimized

displacement of illumination regions is only depending on suns seasonal latitude angle. These effects are not assessed at this stage of work because of the complication of the calculation.

### B. Technical limitations

Modules are often fabricated in dimensions as large as  $800 \times 1500$  mm. For a flat glass no specifications on the relative position of the cells with respect to the glass exist. In the case of waved glass, solar cells must be placed with higher accuracy under the structure of the waved glass as a slight displacement would result a reduction of the efficiency of the module. The positioning accuracy depends on the shape of the waves on the glass and could have a tolerance of about 0.3 mm if the concave shaped waves are 0.5 mm wide as assumed above. This will increase the technical requirements of module manufacturing and thereby their cost, which however is not the main subject of the present work.

## III. SUMMARY AND OUTLOOK

A waved glass cover of solar sells can increase their efficiency by generating a low illumination density in regions over the fingers and a higher illumination between the finger them. In this way it is possible to reduce shadow and resistive losses. The efficiency gain was estimated to 5%, details are presented in table I.

These results are only valid if the illumination source (sun) is perpendicular to the cells i.e. for a sun tracked system. Otherwise the above-mentioned low and high illumination regions will be displaced. In the worst case the illumination region is displaced away from the front contact grid resulting to a reduction in efficiency.

As the majority of terrestrial solar systems are not sun tracked, it would be interesting to estimate the benefits in power generation over a day, i.e. an integration over different positions of the sun. In this context, different shapes and orientations of the waved glass surface should be assessed.

Throughout this work, it was assumed that the light intensity between the fingers is higher when using the waved glass than flat glass. Moreover, it was assumed for simplicity that the light intensity between the fingers is uniformly distributed, which might not be the case in reality. In a more sophisticated model, emitter losses should be calculated according to the light intensity distribution on the surface of the solar cell that corresponds exactly to a particular shape of the waved glass. In this way it is also possible to include more complicated surface structures that minimise the emitter losses by distributing the light in such a way that the regions close to the fingers are more illuminated than between them. In this case the generated current will take a shorter path through the emitter and thereby, emitter losses are further reduced.

### APPENDIX I

#### GEOMETRIC OPTICS ANALYSIS

In this appendix we present some general formulae from geometrical optics needed to calculate the design of the top glass. This then is applied to the two designs presented in figure 3.

The basic notations used in this appendix (cf. also figure 4) are:

- $h(x)$ : Parametrisation of the surface. A one-dimensional situation is considered here, the x-direction agrees with the x-direction in figure 7,  $h(x) = 0$  would imply that the thickness of the glass is zero.
- $\beta$ : Angle between plumb line and in-falling light.
- $\alpha_{i/o}$ : Angle between normal vector and in-falling/outgoing light.
- $\gamma$ : Angle between plumb line and normal vector.

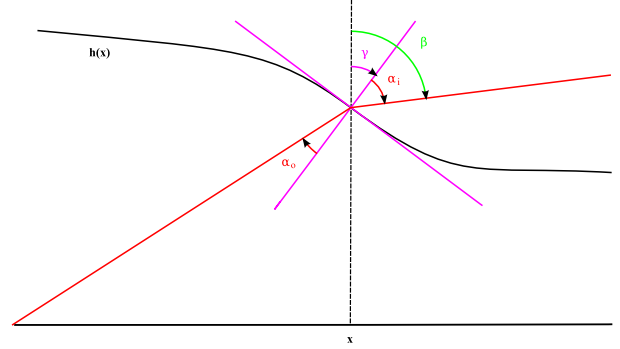


Fig. 4. Basic definition of different angles used in appendix I.

#### A. Basic relations and mapping of the light

All angles are defined by means of the surface parametrisation  $h(x)$ , the angle of the in-falling light and the refraction index of the glass  $N^{-1} \approx 1.5$ :

$$\tan \gamma = -h'(x) \quad \alpha_i = \beta - \gamma \quad \sin \alpha_o = N \sin \alpha_i \quad (1)$$

All angles are measured from the vertex (the direction perpendicular to the plane of the final layer) and positive angles are defined in the clockwise direction, negative in the counter clockwise one.

The notation

$$h(x) = h_0 + \Delta h(x) \quad (2)$$

is useful in many applications, where  $h_0$  is the thickness of the flat glass and  $\Delta h(x)$  the structuring. As  $h_0$  simply is a constant this implies

$$\tan \gamma = -\Delta h'(x) \quad (3)$$

The light has a certain intensity  $\rho$ . On a plane inclined at an angle  $\alpha$  the intensity reduces to  $\rho_\alpha = \rho \cos \alpha$ . Thus the intensity is reduced/augmented due to refraction by

$$\rho_o = \rho \frac{\cos \alpha_i}{\cos \alpha_o} \quad (4)$$

The final layer is again inclined in general, there the in-falling intensity is

$$\rho_f = \rho \frac{\cos \alpha_i}{\cos \alpha_o} \cos(\gamma + \alpha_o) \quad (5)$$

This intensity is mapped upon the point

$$\begin{aligned} z(x) &= x + \Delta z(x) \\ &= x - h(x) \tan(\gamma + \alpha_o) = x - h(x) \frac{\tan \alpha_o - h'}{1 + h' \tan \alpha_o} \end{aligned} \quad (6)$$

The above equations are suitable for a flat surface but do not yet respect changes in the intensity due to a curved surface. From equation (6) an infinitesimal interval  $\delta x = y - x$  is mapped upon

$$\begin{aligned} z(y) - z(x) &= \delta z = \\ &= \delta x \left( 1 - h' \tan(\gamma + \alpha_o) - \frac{h}{\cos^2(\gamma + \alpha_o)} (\gamma' + \alpha'_o) \right). \end{aligned} \quad (7)$$

Despite its complexity the formula easily can be tested in certain limiting cases. In particular for  $N = 1$  the result becomes  $\delta z = \delta x \cos \alpha_i / (\cos \beta \cos \gamma)$ , which is exactly the stretching of the interval due to the angle  $\beta$  of the in-falling light.

With respect to the in-falling light this has to be multiplied by an overall factor  $\cos \gamma / \cos \alpha_i$  and thus the intensity on the final layer as a function of  $x$  becomes

$$\rho_f = \frac{\rho \cos \alpha_i}{\cos \gamma \left( 1 - h' \tan(\gamma + \alpha_o) - \frac{h}{\cos^2(\gamma + \alpha_o)} (\gamma' + \alpha'_o) \right)}. \quad (8)$$

In the case of a flat surface the last term in the denominator vanishes and it is easy to check that the result reduces to (5).

We should mention that we neglect any effects due variations in reflection due to the dependence of Fresnel's equations on the angle of in-falling light. This is justified by the fact that effects should remain negligible up to angles of about  $\pi/6$  for polarised and at least  $\pi/4$  for unpolarised light.

1) *Linearised equations:* Let us consider the case where all angles are small, such that  $\sin \alpha \approx \alpha \approx \tan \alpha$  and consequently  $\cos \alpha \approx 1 - \alpha^2/2$ . This is a good approximation as long as all angles are  $\lesssim \pi/8$ . Then we have

$$\gamma = -h'(x), \quad \alpha_i = \beta + h'(x), \quad \alpha_o = N(\beta + h'(x)). \quad (9)$$

Equation (6) then simplifies to

$$z(x) = x - h(x) (N\beta + (N-1)h'), \quad (10)$$

which yields for  $\delta z$

$$\delta z(x) = \delta x (1 - h' (N\beta + (N-1)h') - (N-1)hh'') \quad (11)$$

and therefore the intensity on the final layer becomes

$$\rho_f = \rho \left( 1 - \frac{\beta^2}{2} + (N-1)h'(\beta + h') + (N-1)hh'' \right). \quad (12)$$

### B. Focal points

Focal points on the final layer might be a technical problem and certainly make the mathematical issues much more involved. Indeed, a focal point on the final layer is indicated by  $z'(x) = 0$ , while  $z'(x) < 0$  means that there exists a focal point between the surface of the glass and the final layer. To avoid focal points on the final layer while assuming a smooth surface of the glass therefore implies the condition

$$z'(x) > 0 \quad \forall x, \quad (13)$$

which at the same time guarantees the invertibility of the function  $z(x)$ .

One can try to estimate the maximal possible curvature of the curve  $h(x)$  in order to avoid focal points on the layer. In the linearised approximation a sphere has the focal length

$$f = \frac{|R|}{1-N}. \quad (14)$$

On the other hand the curvature of the curve  $h(x)$  at the point  $x$  is defined as

$$R = \frac{[1 + (h')^2]^{3/2}}{h''}, \quad (15)$$

whereby  $R > 0$  means that the curve is convex in the point  $x$ . Focal points should be avoided if

$$f > \Delta(x) \quad \forall x \text{ with } R < 0, \quad (16)$$

where  $\Delta(x)$  is the distance the light traverses between entering the glass and hitting the final layer and is most easily expressed as

$$\Delta(x) = h(x) \sqrt{1 + \tan^2(\gamma + \alpha_o)} = \frac{h(x)}{\cos(\gamma + \alpha_o)}. \quad (17)$$

As eq. (14) is valid for small angles only we should impose the same approximation for (17) as well. This yields the relation

$$R > (1-N)h(x) \left( 1 + \frac{1}{2} (N\beta + (N-1)h')^2 \right), \quad (18)$$

or, as a restriction on  $h''$  while noticing that this quantity in the critical case is negative

$$h'' > \frac{(1 + \frac{1}{2}(N\beta + (N-1)h')^2)(1 + (h')^2)^{3/2}}{h(1-N)}. \quad (19)$$

A rough estimate of the size of a typical structure can be given by assuming that the contribution from  $\Delta z$  in (17) is very small and by using the approximation  $h(x) \approx h_0$ . Then we get the relation

$$R > (1-N)h_0. \quad (20)$$

Therefore the maximal region wherefrom light effectively can be focused should be about  $2/3 h_0$ . In the present application we do not expect more than  $1/3 h_0$  for the largest structures and therefore the maximal value for  $\gamma$  should be of the order of  $\pi/3$ , which still is too big for the linear approximation. Therefore for these extreme cases the above calculation actually is not valid.

Instead of working with the radius one can directly analyse the condition

$$z'(x) = 1 + (1-N)(\Delta h'(x))^2 + (1-N)(h_0 + \Delta h)\Delta h'' > 0. \quad (21)$$

In cases where  $z'(x)$  is close to zero the second term clearly is negligible in the range of angles that are acceptable ( $|\gamma| \lesssim \pi/8$ ). Therefore we obtain the simple relation

$$\Delta h''(x) \gtrsim \frac{1}{(1-N)(h_0 + \Delta h)} \approx \frac{3}{h_0}. \quad (22)$$

### C. Analysis of preliminary designs

1) *Avoiding shadow losses altogether:* We present some calculations on a possible design that avoids shadow losses altogether. Its shape is illustrated in figure 3 (top). At the kerb the left limits of the tangents are called  $h'_L$  or  $\gamma_L$ , the limits from the right  $h'_R$  and  $\gamma_R$ .

From this we deduce the two relations

$$(\Delta z)_L = -(K + D), \quad (\Delta z)_R = -(K - D), \quad (23)$$

which can be translated into defining equations for  $\gamma_{L/R}$  ( $h_K$  is the value of  $h(x)$  at the kerb)

$$\frac{K + D}{h_K} = \tan(\gamma_L + \alpha_{oL}) \quad \frac{K - D}{h_K} = \tan(\gamma_R + \alpha_{oR}). \quad (24)$$

Due to the dependence of  $\alpha_o$  on  $\gamma$  in (1) this does not allow a analytic solution even when restricting the values of the angles to the interesting regions.

Restricting to the linear regime we get for  $\beta = 0$

$$h'_L = \frac{K + D}{(N - 1)h_K} \quad h'_R = \frac{K - D}{(N - 1)h_K}, \quad (25)$$

whereby this approximation can be trusted as long as  $h'_{L/R} \lesssim 0.4$ . If we assume  $h_K \approx 3\text{mm}$  and  $N = 2/3$  for glass we obtain

$$K + D \lesssim 0.4\text{mm} \quad |K - D| \lesssim 0.4\text{mm}. \quad (26)$$

How does the shade move once  $\beta \neq 0$ . In the linear regime from (10)

$$z(x)|_{\beta=0} - z(x)|_{\beta} = hN\beta \approx 2\beta, \quad (27)$$

with the same numerical values as above. A numerical analysis shows that the deviations from the linear regime stay small inside the whole range of relevant numeric values.

What is the minimal distance between two fingers. We assume now that  $K > D$  which is the preferable case from a technological point of view. A physical limit is given by the fact that now light from the area between the two kerbs is allowed to hit the shaded region. If other discontinuities shall be avoided a technological limit seems to be the case where (almost) the whole light is focused on the border of the shade. This means that the surface is structured by segments of circles with total width  $2(K + D)$ . The opening angle of the segment clearly is  $2\gamma$  and the radius  $(K + D)/\sin\gamma = |K + D/h'|$ . From this it appears to be feasible to have to fingers in a distance of about 1mm. From this we conclude that these theoretical questions should not be an issue in the design of the surface.

2) *Simpler design:* As discussed in the main part of this paper the design of the previous subsection may be appealing theoretically, but poses some issues in a concrete realisation due to the necessary discontinuity. Here we present some theoretical ideas on the simpler design (bottom of figure 3) that is considered as an alternative.

The basic idea of this simpler design is to spread the light above the fingers and in this way reduce the shadow losses as the illumination of the fingers is reduced. The illumination shall be uniformly be distributed in the area spread. For the

linear case with  $\beta = 0$  this is easily seen to imply an elliptic glass shape from (12). For its parametrisation one obtains from (10) (the bottom of the shape is assumed to be at  $x = 0$ , the total height of the structure denoted by  $\Delta$ ,  $A$  and  $B$  are defined in figure 3)

$$\begin{aligned} h(x) &= \sqrt{(h_0 - \Delta)^2 + \frac{Bx}{N-1} - \frac{\Delta^2 - 2h_0\Delta}{B}x - \frac{x^2}{N-1}}, \\ &= \sqrt{h_0^2 + \frac{2AB - 3B^2}{N-1} - \frac{2A - 4B}{N-1}x - \frac{x^2}{N-1}}. \end{aligned} \quad (28)$$

It should be noted that the linear approximation is valid as long as

$$|A - B| \ll |h_0(N - 1)|. \quad (29)$$

In the application considered in this paper  $A - B \approx 1\text{mm}$  while the glass is about 4mm thick. Therefore one should expect non-linear effects at towards the edges of the structure. Finally notice that the dependence on  $\beta$  to linear order does not depend on the details of the shape of the surface, therefore the same result as in (27) applies here.

## APPENDIX II CALCULATION OF GAIN

In this appendix some details on the calculations of the potential of the proposed concept is presented. The result should help to find the optimum design for a solar cell, in particular the spacing between the fingers for a conventional grid in combination with the use of either a flat glass or a waved glass module. A general methodology is presented to find the ideal spacing of a conventional pattern for given parameters.

Solar cells convert sun light directly into electrical energy. The electrical current is collected by a metallised pattern printed over the surface of the cell (cf. figure 5). The pattern causes a certain loss in energy conversion (typically 7%) associated with its shadow from the bus bars and fingers. Figure 5.A represents a conventional design, on which next calculations will be based on. This design presents the vast majority of solar cells on the market.

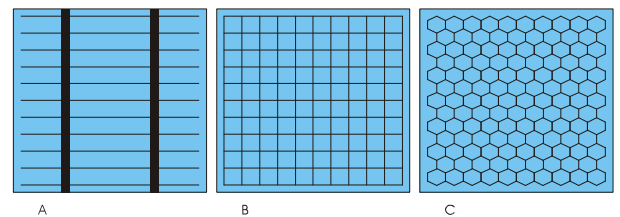


Fig. 5. Different grid designs. A: conventional design; B,C: special designs where the bus bar is transferred to the back side.

The general working principle of a solar cell is illustrated in figure 6. When light is absorbed in the p-n junction electrons and holes are generated, whereby the charges are separated due to the electric field in the junction. Some of these will recombine in the bulk and at the surface edges of the wafer forming a current opposite to the direction of the generated one. A parallel resistor  $R_p$  and a diode  $D$  represent the losses

associated with this current. Further, when the current is collected, Ohmic losses will occur. These are represented by a series resistor  $R_s$ .

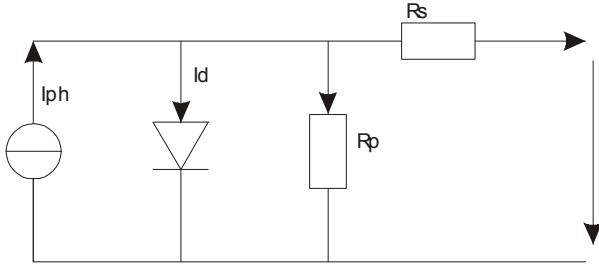
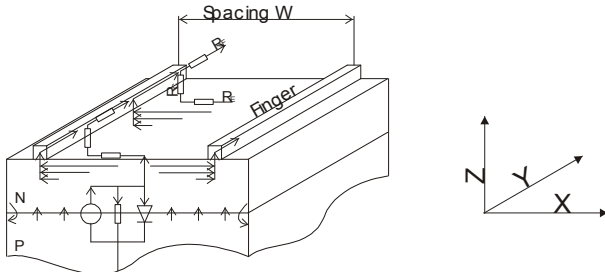


Fig. 6. Equivalent scheme of a solar cell.

The series resistor can be split to the three main components (see figure 7)

- 1) emitter resistance  $R_E$ ,
- 2) contact resistance  $R_C$ ,
- 3) finger resistance  $R_F$ .



The figure illustrates the particular resistances for the Emitter  $R_E$ , the contact  $R_C$  and the finger  $R_F$ .

Fig. 7. 3D view of the solar cell equivalent scheme with some details about the ohmic resistance.

From figure 7 it is obvious that Ohmic resistors and shadow losses are influenced by the geometry of the design and hence the performance of solar cells can be improved by optimising this design.  $R_E$  depends on the spacing between the fingers,  $R_F$  on the cross-section and length of the fingers and  $R_C$  on the contact area and its quality (specific contact resistance). Considering the current flow in the X-axis, it is assumed that the current in the emitter flows in a lateral manner perpendicular to the fingers. A further assumption is that the current is generated uniformly underneath the surface between the fingers. This leads to the conclusion that the current density increases linearly toward the fingers and reaches its maximum under the fingers. Similar conclusions are obtained for the current flow in the direction of the Y-axis. The current is fed in through the contact area (Z-axis) uniformly, while its density increases in the direction of collection (Y-axis).

#### A. Conventional grid design

To calculate the optimal geometry we shall consider the unit cell depicted in figure 8. Its finger length is denoted by  $L$ , the spacing between the centres of the finger by  $W$  and the finger width by  $W_f$ . Since each finger intersects with two unit cells only half of the finger will be considered in the calculation while the bus bar is neglected.

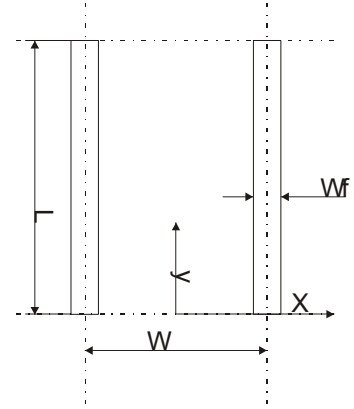


Fig. 8. The design parameters  $L$ ,  $W$  and  $W_f$ .

First we consider the shadow produced by the fingers. It is just ratio of the areas of the fingers and the unit cell:

$$S = \frac{2 \frac{W_f L}{2}}{WL} = \frac{W_f}{W} \quad (30)$$

Next we consider the power losses at the emitter. It is assumed that the current density  $G_c$  [A/cm<sup>2</sup>] is generated uniformly under the area of the unit cell and then directed perpendicularly to the fingers. That means that the current density  $J$  [A/cm] increases in x-direction:  $J = J(x)$ . With the sheet resistance of the emitter  $R_e$  (or its resistivity  $\rho_e$ ) the power loss at any point is

$$P_{l,e}(x) = \rho_e J(x)^2. \quad (31)$$

Due to symmetry reasons  $J(0) = 0$  and  $J(W/2) = G_c W/2$ . The integral of the power loss at the emitter from  $x = 0$  to  $x = W/2$  therefore is

$$P_{l,e} = 2 \int_0^{W/2} \rho_e J(x)^2 dx. \quad (32)$$

In case of a linearly increasing current  $J(x) = G_c x$  as found in this specific example one finds

$$P_{l,e} = \rho_e \frac{G_c^2 W^3}{12}. \quad (33)$$

The total emitter power loss  $P_{l,e,tot}$  in y-direction is the integral of  $P_{l,e}$  over the unit cell:

$$P_{l,e,tot} = \int_0^L P_{l,e} dy = \rho_e \frac{G_c^2 W^3}{12} L \quad (34)$$

Similarly we consider the power losses on the fingers. The current is collected in the direction of the bus bar (Y direction in figure 7), i.e. the current  $I(y)$  increases with increasing finger length  $L$ , where the current entering the finger at any point is  $J(y) = G_c W$ :

$$I(y) = \int_0^L J dy = G_c W \cdot L \quad (35)$$

Introducing the specific resistance of the fingers  $\rho_F$  [Ω/cm] the power loss can be calculated as

$$P_{l,F} = \int_0^L \rho_F I(y)^2 dy = \frac{1}{3} \rho_F G_c^2 W^2 L^3. \quad (36)$$

Finally the power loss over the contact resistance  $R_c[\Omega/\text{cm}^2]$  is considered. Here it is assumed that the current flows only in the z-direction, i.e. from the emitter to the finger, and there is no relevant flow through the contact resistance in the (x,y) plane. This is justified by the fact that the thickness of the contact is very small. Thus, the actual contact resistance can be expressed as

$$R_{c,A} = \frac{R_c}{L_T L}, \quad (37)$$

where the transmission length  $L_T$  instead of line width  $W_f$  has been used as this one is the electric active contact. However, if  $L_T > W_f$ , then  $L_T$  has to be replaced by  $W_f$ . Together with the current from (35) the power losses due to contact resistance becomes

$$P_{l,c} = R_c G_c^2 \frac{W^2}{L_T}. \quad (38)$$

From (34), (36) and (38) it is obvious that the power losses are a function of the spacing  $W$ . In order to keep the shadow at the same ratio when reducing the spacing it is required to reduce the finger width  $W_f$ . But in practise the finger width is limited by the technology, e.g. for screen printed solar cells, the line width typically is between 80 and 120 micrometres. This makes the optimum spacing limited by  $W_f$ . Therefore, the design issue of a conventional grid is always to find the optimal spacing  $W$ .

The total efficiency of the solar cell now can be estimated from subtracting the different losses from the value of an ideal cell. This is

$$P = P_I - P_{l,e} - P_{l,F} - P_{l,c} - P_s \quad (39)$$

where  $P_I$  and  $P_s$  are the ideal power and the shadow losses, resp.,

$$P_I = G_c V_m L W \quad P_s = G_c V_m L W_f \quad (40)$$

### B. Grid design with waved glass

In the case of the waved glass, the concave shape over the fingers distributes a significant part of the light into the active cell area that would otherwise fall on the fingers. For this reason it can be considered that  $W_f$  is reduced by a certain reduction factor  $F_R$ , which is related to the degree to which the concave shape spreads the light, cf. figure 3 (bottom). We define  $F_R$  here as the ratio between the distance  $A$  between the edges of the projected light on the cell and the distance  $B$  between the edges of the waved shape of the glass,  $F_R = B/A$ .

Thus, the loss due to the shadow in the case of the waved glass  $P_{w,s}$  can be considered as

$$P_{w,s} = G_c V_m L (W_f F_R). \quad (41)$$

Thus the result of the waved glass is an effective reduction of  $W_f$  and consequently  $W$  can be reduced as well, which leads to significant reduction of the resistive losses. All other equations from the previous subsection can be considered without modification.

Considering the bus bar, it is assumed that a shape similar to figure 9 is available deflects the light from an area  $C$  over

the bus bar into the active area. In this case a retrieved area  $C \times W$  is created which results in a power gain that can be added to the total power and therefore

$$P = P_I - P_{l,e} - P_{l,F} - P_{l,c} - P_{w,s} + P_G, \quad (42)$$

with

$$P_G = G_c V_m C W. \quad (43)$$

Note that this is a simplified calculation method as we



Fig. 9. The shape of the waved glass over the bus bar

assumed that the current density  $G_c$  is generated uniformly in the area of the unit cell. In the case of waved glass  $G_c$  will not constant as it depends on the radiation density which is not uniformly distributed for most shapes of the waved glass. However, this simplification is justified because the non-uniformity of light affects only the emitter losses, which contributes a relatively small part of the total losses.

### C. Sample calculation

We finally comment on the example presented in table I based on the parameters of table II. It is assumed that  $2B$  (the distance between the edges of the waved shape of the glass) is 0.5mm and while  $2A = 1.5\text{mm}$ , whereby the thickness of the glass is 4mm. The bus bar usually is 2mm wide while  $C$  is assumed to be 0.5mm. For all calculations it is assumed that the light source is orthogonal to the solar cell. For these assumptions the gains presented in table I are obtained.

The solar cells must be placed in a certain position with respect to the waved glass such that the fingers are placed under the area of the modified glass, see figure 3 (bottom). This region 0.5mm for the given example. For the module manufacturer, this presents an acceptable positioning tolerance, thus the requirements on automation and accuracy and thereby its costs are not too high.

It is expected that this method has a lot of advantages compared with alternative technologies where the metallisation grid is partially or completely shifted to the back side of the solar cell. These involve sophisticated technologies and additional presses steps and some drawbacks in solar cells electrical characteristics.

### REFERENCES

- [1] Picture taken from <http://www.specmat.com/pvcells.htm>.
- [2] Picture taken from <http://www.ecn.nl/en/zon/r-d-programme/pv-module-technology/>.